Kinematics Dexterity Analysis and Optimization of 4-UPS-UPU Parallel Robot Manipulator

Guohua Cui*, Haiqiang Zhang, Feng Xu, and Chuanrong Sun

College of Equipment Manufacture,
Hebei University of Engineering,
Handan, Hebei Province, 056038, China
ghcui@hebeu.edu.cn, zhq19860905@126.com

Abstract. The development of a new parallel robot manipulator based on simulation analysis is a rapid approach to discover the unique features or advantage of a conceptual model. In this paper, a 5-DOF parallel robot manipulator which can generate three translations and two rotations was presented. The kinematics mathematical model and Jacobian matrix were derived analytically. The global conditions index (GCI) and the global gradient index (GGI) which represent the evaluation index of dexterity were introduced by considering the kinematics performance indices over the whole workspace. The workspace model of the mechanism was analyzed based on a simplified boundary searching method. The mathematical model of the global condition number was developed simultaneously. The multi-objective optimization model was deduced on the basis of the multidisciplinary design philosophy. The manipulator was optimized by using the design of experiment (DOE) and the multi-island genetic algorithm (MIGA). The optimal solution was chosen from the multi optimal solutions in a reasonable manner. Through the comparison of results before and after optimization, the kinematics performance of the mechanism was improved, which provide not only a guide to the multiple objectives optimal design but also an applicable method of dimensional synthesis for the optimal design of general parallel robot manipulator.

Keywords: Parallel Robot Manipulator, Kinematics Dexterity, Workspace, Multi-objective optimization.

1 Introduction

Parallel manipulator has the advantage of high rigidity, strong bearing capacity, and high precision and small error. Since the Stewart Parallel Manipulator, parallel manipulator has become an international research focus [1][2]. The dexterity and isotropy are of importance performance index to evaluate the mechanism. The kinematics dexterity can evaluate the transmission performance. Gosselin [3]

* This research was supported by the national natural science foundation of China under grant No. 51175143.

X. Zhang et al. (Eds.): ICIRA 2014, Part II, LNAI 8918, pp. 1–11, 2014.
© Springer International Publishing Switzerland 2014

introduced the concept of dexterity into parallel manipulator, and pointed out that the condition of Jacobian matrix can represent the dexterity; Zhang [4] adapted the kinematics condition index (KCI) to evaluated the dexterity, and draw the distribution atlas of spatial KCI; Moreno [5] regarded the condition of Jacobian matrix as the performance index of dexterity, calculated and analyzed the condition. Sergiu [6] proposed a large number of performance criteria dealing with workspace, quality transmission, manipulability, dexterity and stiffness, and the evaluation measures can be used for optimal synthesis; Chen [7] studied the dexterity of 4-UPS-UPU parallel manipulator focused on the seven performance indices; Qi [8] analyzed the structure of the five degree of freedom 4-UPS-UPU and proposed synthesis methods about the operation performance optimization on the orientation workspace.

In this paper, a five degree 4-UPS-UPU parallel manipulator was studied and its kinematics model and the dimensionless Jacobian matrix were established. Considering the kinematics performance on the workspace, the GCI and GGI were introduced as the evaluation index of the dexterity, which was optimized based on the multidisciplinary and multi-objective optimization software Isight. On the basis of workspace, the global condition index was developed and obtained the mathematical model of optimization. Last we obtained the Pareto solution by using design of experiment and multi-island genetic algorithm and selected the reasonable optimal solution. Compared the results before and after optimization, we can draw the conclusion that the new mechanism after optimization has excellent dexterity and transmissions performance, which provide a guide for design optimization and performance assessment. Therefore, it is necessary to seek an effective optimization procedure to improve the performance indices for achieving a higher score evaluation.

2 4-UPS-UPU Parallel Manipulator Model

As shown in Fig.1, 4-UPS-UPU parallel manipulator model and coordinate system were established, which consists of a moving platform, fixed platform and the legs connected the moving platform and the fixed platform, for four identifiable active chains UPS and one constraint active chain UPU, U stands for Hooke joint, P stand for Prismatic joint, S for Spherical joint, where the P joint is driven by a linear actuator.

Suppose that the platforms are circular and the connection points are distributed along the circumference of the moving platform and the fixed platform circles of radii r_a and r_b, respectively. The coordinate system $O-XYZ$ is fixed to the fixed platform and the coordinate $o-xyz$ is attached to the moving platform. x axis point to A_1, z axis perpendicular to the moving platform on the positive axis direction and y axis is given by the right hand. Similarly, X axis point to B_1 point, the Z axis is vertical. The points of intermediate branched Hooke joints are located on the point o and point O of the moving platform and the fixed platform, respectively.

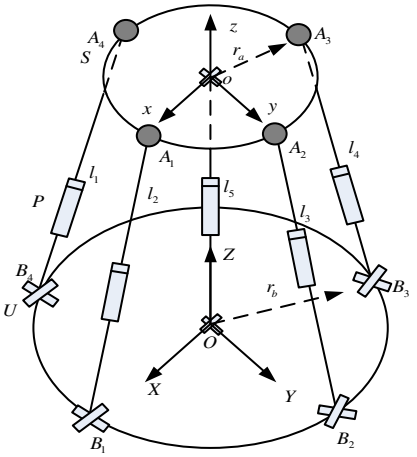

Fig. 1. The schematic diagram of 4-UPS-UPU parallel manipulator architecture

The number of degree of freedom for the parallel manipulator can be obtained by the general Kutahach-Grubler formula [9]

$$M = \mathrm{d}(n-g-1)+\sum_{i=1}^{g} f_i = 6\times(12-15-1)+29 = 5 \tag{1}$$

The 4-UPS-UPU parallel manipulator is a spatial 5-DOF, its moving platform can move in X , Y , Z and rotate around X and Y direction.

3 4-UPS-UPU Parallel Manipulator Kinematics Model

3.1 Inverse Kinematics Solution

As shown in Fig.1, position vector A_i , B_i and branched chains A_iB_i , for $i = 1,2,3,4$, the Cartesian coordinate of the moving platform is given by the position vector ${}^{O}A_i$ with respect to the moving coordinate system, and the position of the attachment point B_i with respect to the fixed coordinate system can be written as ${}^{O}B_i$. The Cartesian variables are chosen to be the relative position and orientation of $o-xyz$ frame with respect to $O-XYZ$ frame, where the position of o is specified by the position of its origin with respect to $O-XYZ$ frame, Furthermore, if vector $o=\begin{bmatrix} x & y & z \end{bmatrix}^T$ described the position of the attachment point o with respect to $O-XYZ$ frame. The coordinate can be represented as following,

$${}^{o}A_i = \begin{bmatrix} A_{ix} & A_{iy} & A_{iz} \end{bmatrix}^T ,$$

$${}^{O}B_i = \begin{bmatrix} B_{iX} & B_{iY} & B_{iZ} \end{bmatrix}^T ,$$

$${}^{O}A_i = \begin{bmatrix} A_{iX} & A_{iY} & A_{iZ} \end{bmatrix}^T$$

${}^{O}A_i$ is expressed with respect to the coordinate system $O-XYZ$ can be computed by

$$ {}^{O}A_i = Q\,{}^{o}A_i + o \tag{2}$$

Q is a matrix describing the orientation of $o-xyz$ with respect to the $O-XYZ$, here RPY coordinate system representation is chosen to describe the pose, that is ,

$$ Q = \begin{bmatrix} c\beta & s\alpha s\beta & c\alpha s\beta \\ 0 & c\alpha & -c\alpha \\ -s\beta & s\alpha c\beta & c\alpha c\beta \end{bmatrix} \tag{3}$$

Where, s and c present sine and cosine, respectively
The length vector can be expressed as

$$ L_i = A_iB_i = {}^{O}A_i - {}^{O}B_i \tag{4}$$

Then, the length of the active leg can be expressed by taking the norm of the vector of Eq.(4), we can get the

$$ l_i = \left\| A_iB_i \right\| = \left\| {}^{O}A_i - {}^{O}B_i \right\| \tag{5}$$

3.2 Jacobian Matrix of the Parallel Manipulator

The relation between active joint velocities $\dot{l} = \begin{bmatrix} \dot{l}_1 & \dot{l}_2 & \dot{l}_3 & \dot{l}_4 & \dot{l}_5 \end{bmatrix}^T$ and twist of the end-effector $t = \begin{bmatrix} \dot{x} & \dot{y} & \dot{z} & \omega_x & \omega_y \end{bmatrix}^T$ can be described using a differential kinematics model, namely,

$$ \dot{l} = \mathbf{J}t \tag{6}$$

Where **J** denote the Jacobian matrix

$$ \mathbf{J} = \begin{bmatrix} q_1 & q_2 & q_3 & q_4 & q_5 \\ r_1 \times q_1 & r_2 \times q_2 & r_3 \times q_3 & r_4 \times q_4 & r_5 \times q_5 \end{bmatrix}^T = [\mathbf{J}_1 \vdots \mathbf{J}_2] \tag{7}$$

Where, the unit vector q_i, for $i = 1,2,3,4,5$ can be expressed in terms of position vectors, namely,

$$ q_i = \frac{L_i}{l_i} \tag{8}$$

And vector r_i can be written as

$$ r_i = Q\,{}^{o}A_i \tag{9}$$

$\mathbf{J}_1$ denoted Jacobian matrix of linear velocity and $\mathbf{J}_2$ denoted Jacobian matrix of angle velocity , whose dimension of $\mathbf{J}_1$ and $\mathbf{J}_2$ are both 6×3. Considering the unit

difference of the Jacobian matrix was dimensionally inhomogeneous [10]. So we use a characteristic length, L_c, to homogenize the original Jacobian matrix in such a way that

$$\mathbf{J}_H = \mathbf{J} \cdot diag(1,1,1,\frac{1}{L_c},\frac{1}{L_c},\frac{1}{L_c}) \tag{10}$$

Where, $L_c = \sqrt{\frac{trace(J_2^T J_2)}{trace(J_1^T J_1)}}$ and $\mathbf{J}_H$ denotes the new homogeneous Jacobian matrix.

4 Performance Index of Kinematics Dexterity

In order to make the mechanism has good kinematics performance in the workspace, the kinematics dexterity optimization was studied and the GCI and the GGI were introduced as the evaluation index [11].

4.1 The Global Condition Index

The condition number of the Jacobian matrix changed along with the position and orientation of parallel robot manipulator, therefore, it cannot be measured the dexterity of the mechanism in the whole workspace. In order to obtain the kinematics performance in the whole workspace, Gosselin and Angeles [12] proposed the global condition index, which is a measure of its kinematics precision and control accuracy and which is defined as the ratio of the integral of the inverse condition numbers calculated in the whole workspace, dived by the volume of the workspace, i.e.,

$$GCI = \frac{\int_W \nu dW}{\int_W dW} \tag{11}$$

In which ν is the local condition number defined as the reciprocal of the condition of the Jacobian matrix at a particular pose, and W is the workspace. It is noteworthy that the Global Condition number Index is bounded as (0, 1). If the GCI approach zero, the mechanism has a bad global performance and as the GCI approaches one the mechanism has a good global performance. Therefore, we should make the optimization objective GCI maximization.

4.2 The Global Gradient Index

The global gradient index reflected the average deviation level of the kinematics performance in the working space, and cannot reflect the fluctuation properties of mechanism in the working space. F.A.Lara-Molina [13] proposed the global gradient index, which represented the fluctuation information of the local performance index, and defined as

$$\nabla GGI = \max_W \left\| \nabla 1 / \kappa(J) \right\| \tag{12}$$

Where, the local gradient condition number can be expressed as

$$\nabla 1/\kappa = [\frac{\partial 1/\kappa(J)}{\partial x}, \frac{\partial 1/\kappa(J)}{\partial y}, \frac{\partial 1/\kappa(J)}{\partial z}, \frac{\partial 1/\kappa(J)}{\partial \alpha}, \frac{\partial 1/\kappa(J)}{\partial \beta}] \tag{13}$$

GGI is approximately equal to the maximum value of the local gradient throughout the workspace. As the gradient is bigger, so the fluctuation of the kinematics dexterity is greater. That means the kinematics performance of the parallel robot manipulator is up and down in the entire workspace. If the gradient is small, the kinematics performance of the mechanism in the working space is more stable. Therefore, the global gradient index should take the smallest value in the whole working space.

4.3 The Workspace Analysis

The workspace of parallel robot manipulator can be divided into constant orientation workspace and the dexterous workspace. Because of rotation around z axis constrained by the institution, so the mechanism doesn't have the dexterous workspace. In this paper, we established the GCI based on the constant orientation workspace, according the Section 4.1, we need to solve the workspace [14]. The workspace can be expressed as

$$W = \{(x, y, z) \in R \mid f(x, y, z) \le 0\} \tag{14}$$

Where, $f(x, y, z) \le 0$ denoted the constraint condition, namely,

(1) The active chains length constraints can be expressed by

$$1_{\min} \le l_i \le l_{\max} \tag{15}$$

Where $l_{\max}$ denoted the maximum link length, l_i denoted the link length of the i th link, and $1_{\min}$ denoted the minimum link length;

(2) The rotational angle of the spherical joint and the Hooke joint and their constraint can be computed by

$$\theta_u = arcc\cos(l_i \bullet eb / \|l_i\|) \le \theta_{u\max} \tag{16}$$

$$\theta_s = arc\cos(l_i \bullet ea / \|l_i\|) \le \theta_{s\max} \tag{17}$$

Where, ea, eb represented the unit normal vector of the moving platform and fixed platform, respectively. $\theta_{u\max}$, $\theta_{s\max}$ represented the max angle limitation of the Hooke joint and Spherical joint, respectively.

(3) The mechanism was non-singular configuration, namely, the determinant of the Jacobian matrix was not equal to zero.

In order to obtain the position workspace of 4-UPS-UPU parallel manipulator quickly, we set the structural parameters of the parallel robot manipulator as, respectively: the circumcircle radius of the moving platform $r_a = 0.06$ m, the circumcircle radius of the fixed platform $r_b = 0.15$ m, the maximum shrinkage limit of the active chains are 0.05 m ,the maximum elongation limit is 0.25 m , the maximum

angle of the Hooke joint and the Spherical joint are both $\frac{\pi}{3}$. The translation ranges of the moving platform when $\alpha=\beta=0^{\circ}$ are $x\in[-0.1m,0.1m]$, $y\in[-0.1m,0.1m]$, $z\in[0.05\text{m},0.2\text{m}]$. The workspace is drawn using software MATLAB, as shown in Fig.2.

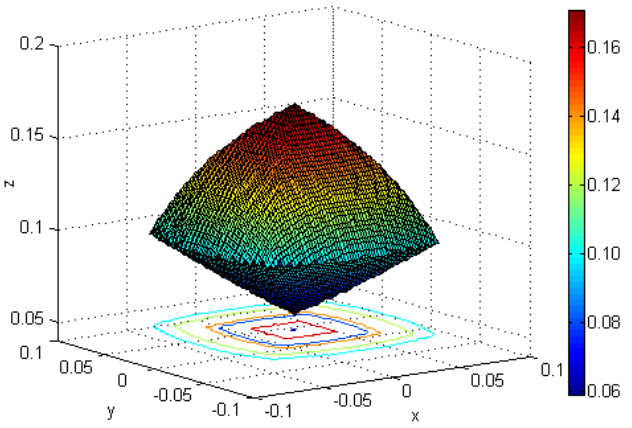

Fig. 2. Workspace of the 4-UPS-UPU parallel manipulator

5 The Multi-objective Optimization Problem of 4-UPS-UPU Parallel Robot Manipulator

5.1 The Optimization Model

The scale parameters of the parallel manipulator were radii of the moving platform r_a and the fixed platform r_b. Select the link length of the active chains l_i, and angle of the Hooke joint θ_u and Spherical joint θ_s as the constraint conditions, the optimization objective functions for GCI and the GGI, then the multi-objective optimization model can be expressed as

$$\begin{cases}\max f_1 = GCI(r_a,\ r_b)\\ \max f_2 = -GGI(r_a,\ r_b)\end{cases} \tag{18}$$

$$\text{s.t.}\ \begin{cases}0.03\le r_a\le 0.08\\ 0.08\le r_b\le 0.18\\ 0.05\le l_i\le 0.325\\ \theta_s\le\dfrac{\pi}{3}\\ \theta_u\le\dfrac{\pi}{3}\end{cases} \tag{19}$$

5.2 The Optimization Results Analysis

Isight software integrated MATLAB, which adopted design of experiment and optimal algorithm to solve the maximum value of *GCI* and the minimum value of *GGI* [15]. The design of experiment (DOE) used the optimal Latin hypercube method and optimal algorithm used multi island genetic algorithm (MIGA).
Genetic algorithm parameters configuration are as follows:

Total population size: 100;
Sub population number: 10;
The number of the island: 20;
The total number: 100;
Cross probability: 0.8;
Migration rate: 0.45;
Interval algebra migration: 5;
The ratio of the individual to participate competition: 1;
The number of elite individuals of the next generation: 1;

In the multi-objective optimization process based on Isight, the samples points in the design of experiment were calculated and eliminated the values which were inconsistent with the constraints, and the values which were satisfied the constraints would access to the optimization part and conducted the multi-objective optimization solution. After several genetic iterations, we can obtain the Pareto frontier of the GCI and the GGI.

We can obtain the main effect diagram and Pareto diagram between design variables and objective functions from the design of experiment, as shown in Fig.3 to Fig.6. We can get the Pareto frontier between the GCI and the GGI and the feasibility of the design of optimization at the end of the MIGA optimization, in the following Fig.7 and Fig.8.

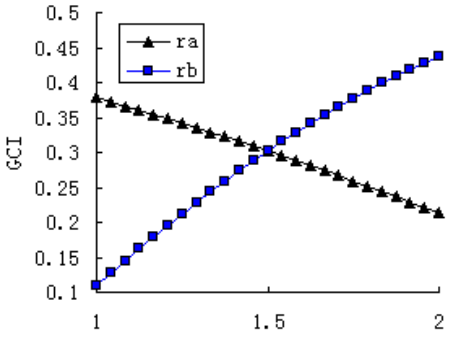

Fig. 3. The main effect between the design variables and GCI

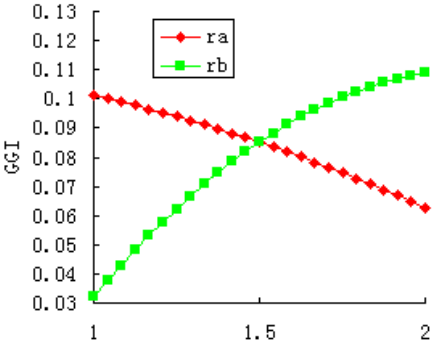

Fig. 4. The main effect between the design variables and GGI

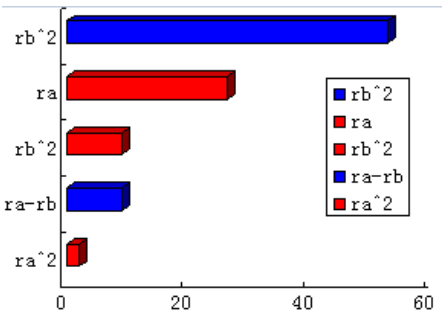

Fig. 5. Pareto diagram of the Global Condition Index

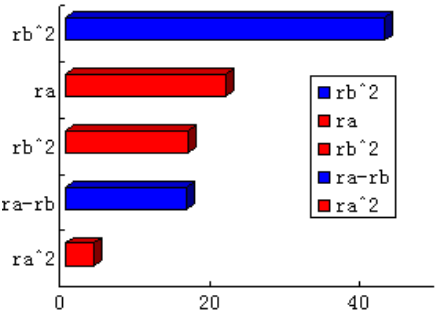

Fig. 6. Pareto diagram of the Global Gradient Index

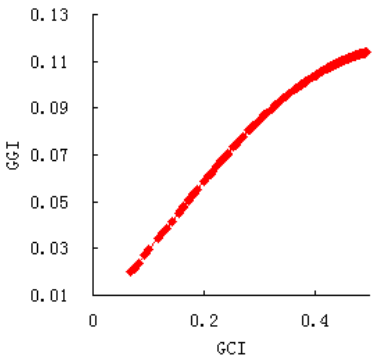

Fig. 7. Pareto frontier of the global performance indices

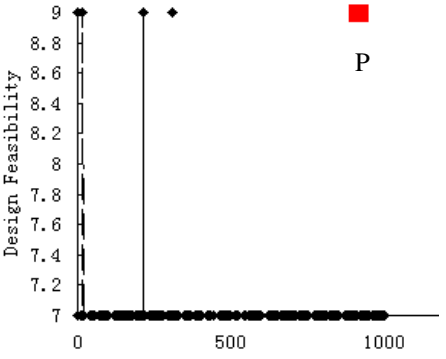

Fig. 8. The feasibility of the optimal design

As is shown in the Fig.3 and Fig.4 above, we can see that the design variables r_a and r_b have a large effect on the global performance indices GCI and GGI, and there is a linear relationship. From Fig.5 and Fig.6, r_b^2, the square of the design r_b, has a big contribution to GCI approximately sixty percent (the blue denoted the positive effect). Secondly, r_a has a big impact on the performance GGI (the red denoted the negative effect). The cross term $r_a - r_b$ has a small effect on the GCI. The influence trend of the design variables is substantially the same between GCI and GGI. Distribution from the Pareto solution in Fig.7, we can see that the Global Condition Index and the Global Gradient Index were the conflicting indices. If the GCI increased, simultaneously, the GGI would improve. Multi-objective optimization was different from the single objective optimization, not to obtain a solution of the function. Due to the conflicting of the multi-objective function, the Pareto solution may not be dominant. But if we simply optimize a target, we may make the other performance index poor.

As can be seen in Fig.8, the feasibility of the optimization design was more than seven, which indicated it was feasible to optimization design. What's more, the red box represented the recommended design point. In this paper, we choose P point as the optimal solution, and the best variables are revealed in Table 1 (Fig.8).

Table 1. Results comparison before and after optimization

	r_a	r_b	*GCI*	*GGI*
Before optimization	0.06	0.15	0.28	0.08
After optimization	0.044	0.198	0.46	0.1

The result shows that the kinematics dexterity increased, but loss the gradient index. So the designers need to weigh the results according to the specific application.

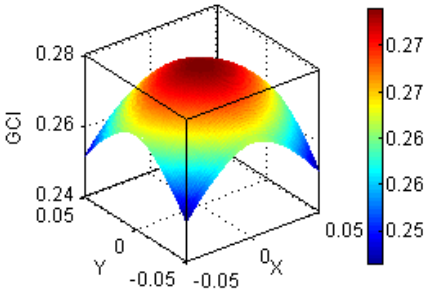

Fig. 9. Local dexterity before optimization when $z = 0.08$

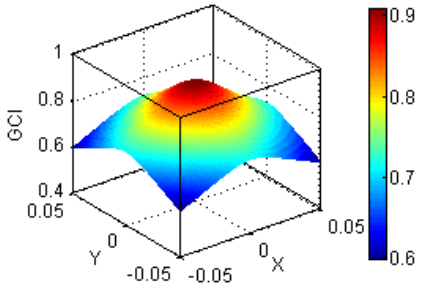

Fig. 10. Local dexterity after optimization when $z = 0.08$

Through the comparisons between Fig.9 and Fig.10, we can see the kinematics dexterity increased obviously after optimization, in the position $x = 0$, $y = 0$, $z = 0.08$, has the best dexterity, and the value is close to one. Due to the symmetry of the mechanism, the dexterity was also symmetric distribution in the workspace. By weighing comprehensively, we can choose P point as the design optimization solution.

6 Conclusion

(1) In this paper, 4-UPS-UPU parallel manipulator with a five-degree of freedom was studied, and the kinematics model and the Jacobian matrix were established. Considering the kinematics performance in the workspace, we introduced the GCI and the GGI as the evaluation criterion of the kinematics dexterity.

(2) We established a mathematical model of the global index on the workspace; and we constructed the multi-objective optimization model of 4-UPS-UPU parallel manipulator. In order to obtain the global performance value, we must solve the workspace firstly.

(3) Multi-objective optimization research was conducted on the basis of the multidisciplinary design optimization software Isight, adopted the design of experiment and the multi-island genetic algorithm to optimize the 4-UPS-UPU parallel manipulator, and obtained the Pareto solutions.

(4) We choose the optimal solution from the number of the solutions in reasonable selection and determined the structural parameters and optimization parameters. The results between before and after optimization show that the kinematics performance improved highly. The methodology in this paper paves the way for providing not only the effective guidance but also a new approach of dimensional synthesis for the optimal design of general parallel mechanisms.

References

1. Gupta, A., O'Malley, K., Patoglu, V., et al.: Design, Control and performance of Rice Wrist: A Force Feedback Wrist Exoskeleton for Rehabilitation and Traning. The International Journal of Robotics Research 27(2), 233–251 (2008)
2. Refaat, S., Herve, J., Nahavandi, S.: Two-mode overatrained three-DOFs rotational translational linear motor based parallel-kinematics mechanism for machine tool application. Robotic 25, 461–466 (2007)
3. Gosselin, C.: Dexterity indices for planar and spatial robotic manipulators. In: 1990 IEEE International Conference Robotics and Automation, vol. 1, pp. 650–655 (1990)
4. Zhang, Y., Zhang, H.: Kinematics and Dexterity Analysis of a Novel Pure Translational Parallel Manipulator. Machine Tool and Hydraulics 08, 13–16 (2010)
5. Moreno, H.A., Pamanes, J.A., Wenger, P., et al.: Global optimization of performance of a 2PRR parallel manipulator for cooperative tasks. In: 3rd International Conference on Informatics in Control, Automation and Robotics (2006)
6. Stan, S., Manic, M., Szep, C., et al.: Performance analysis of 3DOF Delta parallel. In: 2011 4th International Conference on Human System Interaction (HSI), Yokohama, Japan, May 19-21 (2011)
7. Chen, X., Gao, Q., Zhao, Y.: Research on Dexterity Measures of 4-ups-upu Parallel Coordinate Measuring Machine. Computer Integrated Manufacturing System 18(6) (2012)
8. QI, M.: Dimensional synthesis of 4-UPS/UPU 5-DOF parallel mechanism. Journal of Harbin Institute of Technology 11(41), 160–164 (2009)
9. Yu, J., Liu, X., et al.: The robot mechanism mathematical foundation. Mechanical Industry Press (2008)
10. Xie, B., Zhao, J.: Advances in Robotic Kinematic Dexterity and Indices. Mechanical Science and Technology 08, 1386–1393 (2011)
11. Gosselin, C., Angeles, J.: A Global Performance Index for the Kinematic Optimization of Robotic Manipultors. Journal of Mechanical Design 113(3), 220–226 (1991)
12. Gosselin, C., Angeles, J.: The optimum kinematics design of a spherical three degree of freedom parallel manipulator. ASME Journal of Mechanisms, Transmissions, and Automation in Design 111(2), 202–207 (1989)
13. Lara-Molina, F.A., Rosario, J.M., et al.: Multi-Objective design of parallel manipulator using global indices. The Open Mechanical Engineering Journal 4, 37–47 (2010)
14. Cui, G., Zhou, H., Wang, N., et al.: Multi-objective Optimization of 3-UPS-S Parallel mechanism Based on Isight. Journal of Agricultural Machinery 09, 261–266 (2013)
15. Stan, S.D., Manic, M., Măties, M., Bălan, R.: Evolutionary Approach to Optimal Design of 3 DOF Translation Exoskeleton a Medical Parallel Robots. In: HSI 2008, IEEE Conference on Hum System Interaction, Krakow, Poland, May 25-27 (2008)